Nitrite-derived nitric oxide reduces hypoxia-inducible factor 1α-mediated extracellular vesicle production by endothelial cells

Nicholas Burnley-Hall[1*], *Gareth Willis*[2*], *Jessica Davis*[3], *D. Aled Rees*[4], *Philip E. James*[5].

[1]School of Medicine, Cardiff University, Cardiff, CF24 4HQ

[2]Division Newborn Medicine, Boston Children's Hospital, Harvard Medical School, Harvard University, Boston, USA, MA 02115.

[3]Institute of Cancer & Genetics, Cardiff University, Cardiff, UK, CF14 4XN

[4]Neurosciences and Mental Health Research Institute, School of Medicine, Cardiff University, Cardiff, UK, CF24 4HQ

[5]Cardiff School of Health Sciences, Cardiff Metropolitan University, Cardiff, CF5 2SG

*Authors contributed equally to this work.

Running title: Nitric oxide reduces vesicle production in hypoxia.

Correspondence address and request for reprints to: Professor Philip James

Cardiff School of Health Sciences, Cardiff Metropolitan University, Cardiff, CF5 2YB

Email: PJames@cardiffmet.ac.uk Telephone: +44 02920 417129

Highlights

- Hypoxia-inducible factor 1α, but not 2α, mediates extracellular vesicle release in endothelial cells
- Nitrite-derived nitric oxide increases HIF-1α degradation, and subsequently reduces extracellular vesicle production
- This effect is attenuated by inhibition of xanthine oxidoreductase, preventing the conversion of nitrite to nitric oxide.

Summary

Introduction: Extracellular vesicles (EVs) are small, spherical particles enclosed by a phospholipid bilayer (~30-1000nm) released from multiple cell types, and have been shown to have pathophysiological roles in a plethora of disease states. The transcription factor hypoxia-inducible factor-1 (HIF-1) allows for adaptation of cellular physiology in hypoxia and may permit the enhanced release of EVs under such conditions. Nitric oxide (NO) plays a pivotal role in vascular homeostasis, and can modulate the cellular response to hypoxia by preventing HIF-1 accumulation. We aimed to selectively target HIF-1 via sodium nitrite ($NaNO_2$) addition, and examine the effect on endothelial EV, size, concentration and function, and delineate the role of HIF-1 in EV biogenesis.

Methods: Endothelial (HECV) cells were exposed to hypoxic conditions (1% O_2, 24 hours) and compared to endothelial cells exposed to normoxia (21% O_2) with and without the presence of sodium nitrite ($NaNO_2$) (30 μM). Allopurinol (100 μM), an inhibitor of xanthine oxidoreductase, was added both alone and in combination with $NaNO_2$ to cells exposed to hypoxia. EV and cell preparations were quantified by nanoparticle tracking analysis and confirmed by electron microscopy. Western blotting and siRNA were used to confirm the role of HIF-1α and HIF-2α in EV biogenesis. Flow cytometry and time-resolved fluorescence were used to assess the surface and intravesicular protein content.

Results: Endothelial (HECV) cells exposed to hypoxia (1% O_2) produced higher levels of EVs compared to cells exposed to normoxia. This increase was confirmed using the hypoxia-mimetic agent desferrioxamine. Treatment of cells with sodium nitrite ($NaNO_2$) reduced the hypoxic enhancement of EV production. Treatment of cells with the xanthine oxidoreductase inhibitor allopurinol, in addition to $NaNO_2$ attenuated the $NaNO_2$-attributed suppression of hypoxia-mediated EV release. Transfection of cells with HIF-1α siRNA, but not HIF-2α siRNA, prior to hypoxic exposure prevented the enhancement of EV release.

Conclusion: These data provide evidence that hypoxia enhances the release of EVs in endothelial cells, and that this is mediated by HIF-1α, but not HIF-2α. Furthermore, the reduction of NO_2^- to NO via xanthine oxidoreductase during hypoxia appears to inhibit HIF-1α-mediated EV production.

Key words: Extracellular vesicles, hypoxia, hypoxia-inducible factor, nitrite, nitric oxide

Abbreviations

Extracellular vesicles (EVs)

Hypoxia-inducible factor 1 (HIF-1)

Nitrate (NO_3^-)

Nitrite (NO_2^-)

Nitric oxide (NO)

Nanoparticle tracking analysis (NTA)

Sodium nitrite ($NaNO_2$)

Time-resolved fluorescence (TRF)

1. Introduction

The production of extracellular vesicles (EVs) is a common feature of eukaryotic cells, including platelets, leukocytes, and endothelial cells [1]. EVs are spherical, submicron structures enclosed by a phospholipid bilayer, containing a variety of proteins, mRNAs and microRNAs [2]. Their application to modulate physiology is complex, with evidence for them both augmenting and alleviating disease, depending on their cellular origin and subsequent biophysical composition [3]. Elevated levels of EVs have been shown to have pathophysiological roles in a plethora of disease states, including cancer [4–6], neurodegenerative disorders [7–10], and cardiovascular disease [11–13]. Specifically, endothelial cell derived EVs have been shown to express tissue factor, suggesting a role in augmenting the coagulation cascade [14]. Additionally, EVs from patients with myocardial infarction have been shown to induce endothelial dysfunction *ex vivo* [15]. It has recently been shown that endothelial cells enhance EV secretion following temporary hypoxia exposure *in vivo* [16,17], a fundamental feature of the aforementioned diseases and resulting pathologies [18–20]. Indeed, EVs derived from endothelial cells exposed to hypoxia have been shown to produce a markedly altered RNA and protein composition, although the function of these EVs remains undetermined [21].

The adaptation of cellular physiology in response to hypoxia is largely mediated by the transcription factor hypoxia-inducible factor (HIF)-1, which promotes the transcription of genes involved in cell proliferation, metastasis, angiogenesis, and vascular remodelling [22,23]. HIF is comprised of an oxygen regulated HIF-α subunit (HIF-1α or HIF-2α) and the constitutively expressed HIF-1β. Whilst HIF-1α is ubiquitously expressed, HIF-2α is detected predominantly in vascular endothelial cells [24]. The HIF-α subunit is targeted for degradation under normoxic conditions by the O_2-dependent HIF-α prolyl hydroxylase enzymes. These enzymes hydroxylate two conserved prolyl residues (Pro 564 and Pro402) in the central oxygen-dependent degradation domain of the HIF-α subunit (both HIF-1α and HIF-2α), which promotes the binding of the Von Hippel-Lindau protein, allowing ubiquitination and subsequent degradation [25,26]. Inhibition of these enzymes in hypoxia prevents the degradation of HIF-α, allowing regulation of its transcriptional target genes [25]. HIF has been shown to increase expression of several proteins involved in cytoskeletal changes [27], a mechanism thought to be implicated in augmented EV release [28]. Thus, selective targeting and modulation of HIF-α could modulate endothelial cell EV release.

Endothelial-derived nitric oxide (NO) plays a pivotal role in vascular homeostasis, highlighted by the deficiency of NO prevalent in cardiovascular disease states [29]. NO can modulate the cellular response to hypoxia by preventing the stabilization of HIF-α via an increase in prolyl hydroxylase-mediated degradation [30,31]. Previously, impaired endogenous NO production in HUVECs has been shown to increase EV formation [32]. Recently, the inorganic anions nitrate (NO_3^-) and nitrite (NO_2^-),

once thought to be inert end products of NO metabolism, have been shown to be bioactive reservoirs for NO bioactivity, particularly during hypoxia [33,34]. NO_3^- is reduced to NO_2^- via commensal bacteria present in the oral cavity. NO_2^- can subsequently be reduced through reaction with various proteins that possess NO_2^- reductase activity, including Xanthine Oxidoreductase (XOR) [35,36], heme globins [37,38], and components of the mitochondrial electron transport chain [39,40].

Here, we aimed to elucidate the role of both HIF-1α and HIF-2α in endothelial EV release, and selectively target their expression in hypoxia via sodium nitrite ($NaNO_2$) addition, and investigate the effect on endothelial cell EV production.

2. Methods

2.1 Cell culture & viability

Human (HECV) endothelial cells were purchased from Interlab Cell Line Collection (ICLC, Naples, Italy). This cell line was used as a convenient model of endothelial cell behaviour. HECVs were maintained in Dulbecco's Modified Eagle Medium (DMEM, PAA Laboratories Ltd, UK) supplemented with 10% foetal calf serum (FCS, PAA Laboratories Ltd, UK), and 1% penicillin/streptomycin (P/S, Gibco®, Life Technologies, UK). Human umbilical vein endothelial cells (HUVECs) were isolated from umbilical cords as previously described [41]. Human umbilical cords were obtained from the Antenatal Clinic, University Hospital Wales. Ethical approval was obtained from the Research Ethics Committee (REC) (REC reference: 14/NW/1459). HUVECs were maintained in M199 medium, supplemented with 10% foetal calf serum, 1% penicillin/streptomycin, human epidermal growth factor (1 ng/mL, Invitrogen, UK) and hydrocortisone (1 ng/mL, Sigma-Aldrich, UK). HUVECs were used at passage 0 and not sub-cultured. Cells were cultured using T25 cm^2 flasks (Cellstar®, Greiner Bio-One, Germany) and maintained in an incubator at 37 °C and 5% CO_2. Cell counts were undertaken using trypan blue exclusion (1:1 v/v) and a Cellometer Auto T4 (Nexcelom Biosciences, USA). Cell viability and apoptosis were determined using MTS and Caspase-Glo 3/7 assays (Promega, Southampton, UK), respectively, according to the manufacturers' instructions.

2.2 Hypoxia exposure

Hypoxic experiments were performed using an I-CO_2N_2 regulated InVivo 400 hypoxia workstation (Ruskinn, Bridgend, UK). Upon cells reaching ~80% confluency, culture medium was removed. HECVs were washed with phosphate-buffered saline (PBS) (Fisher Scientific, UK) and incubated with 10 mL EV-free serum free medium (SFM) for 24-hours. Cells were cultured at either normoxia (21% O_2, 5% CO_2, 37 °C) or hypoxia (1-20% O_2, 5% CO_2, 37 °C). The hypoxia mimetic agent desferrioxamine was added (100 μM) to HECVs incubated in normoxia to confirm the role of hypoxia in EV formation.

2.3 Extracellular vesicle isolation

EVs were isolated direct from cell culture as previously described [42]. Cells were cultured in serum-free medium (SFM) for 24 hours prior to EV isolation to avoid contamination from foetal calf serum. Cell culture medium was extracted direct from the culture flask and subjected to differential ultra-centrifugation. Culture medium was spun at 500 × *g* for 10 min to remove any cells in suspension. The supernatant was then centrifuged at 15,000 × *g* for 15 min to remove any cell debris. Finally,

supernatants were ultracentrifuged at 100,000 × *g* for 60 min to pellet EVs. This pellet was then resuspended in 1 x sterile PBS, stored at 4°C and analysed within 1 week of isolation.

2.4 EV size and concentration analysis

Size and concentration distributions of EVs were determined using nanoparticle tracking analysis (NTA, NanoSight LM10 system, UK) as described previously [43]. NTA is a laser illuminated microscopic technique equipped with a 642 nm laser and a high sensitivity digital camera system (OrcaFlash2.8, Hamamatsu, NanoSight Ltd) that determines the Brownian motion of nanoparticles in real-time to assess size and concentration. Sixty-second videos were recorded and particle movement was analysed using NTA software (version 2.3). Camera shutter speed was fixed at 30.01 ms and camera gain to 500. Camera sensitivity and detection threshold were (11–14) and (4–6), respectively. A representative NTA trace can be seen in Appendix Figure A1. EV samples were diluted in EV-free sterile water (Fresenius Kabi, Runcorn, UK). Samples were run in quintuplicate, from which EV distribution, size and average concentration were calculated. EV concentrations were then normalised to cell count and expressed as EVs/cell.

2.5 Silencing RNA (siRNA) transfection

siRNA specific for HIF-1α (Dharmacon SMARTpool, UK) was mixed with siRNA transfection reagent (Dharmacon RNAi Technologies) at a ratio of 20:1 and incubated at room temperature for 20 minutes. This mix was added to the medium of ~50% confluent HECV cells to give a final concentration of 100 nM per flask. Control experiments consisted of transfection with the ON-TARGETplus non-targeting siRNA control (100 nM; Dharmacon RNAi Technologies). Cells were incubated in medium containing either HIF-1α siRNA or control siRNA for 48-72 hours prior to hypoxia exposure for 24 hours.

For HIF-2α silencing, the siRNA duplex was mixed with siRNA transfection reagent (Santa Cruz Biotechnology, USA) (1:1 ratio) in transfection medium and incubated at room temperature for 30 minutes before being added onto the cells. Cells were incubated for 5 hours before 2x DMEM (20% FCS, 2% P/S) was added. Cells were incubated for an additional 24 hours before replacing the medium with fresh 1x DMEM (10% FCS, 1% P/S). Cells were incubated for an additional 48-72 hours prior to hypoxia exposure for 24 hours.

2.6 Nitrite treatment and xanthine oxidoreductase inhibition

Preliminary experiments established a $NaNO_2$ dose-effect curve (0.3-300 μM) where 30μM was discovered to be the optimal dose and was used for all subsequent experiments (Appendix Figure A2). Cells were incubated in either hypoxia (1% O_2), or normoxia for 24-hours. Allopurinol (100 μM) was added to inhibit the hypoxia mediated reduction of NO_2^- to NO by xanthine oxidoreductase in HECVs

exposed to hypoxia for 24 hours. The NO donor S-Nitrosoglutathione (GSNO, 10 µM) was also added to cells to confirm the effect of NO on EV production.

2.7 Western blot

HECVs were washed with phosphate-buffered saline (PBS) and lysed in ice-cold Pierce® RIPA lysis buffer (ThermoFisher, UK). The lysates underwent centrifugation at 13,000 x *g* for 20 min at 4 °C. The supernatants were collected and their protein concentrations were determined by a Pierce® BCA Protein Assay Kit (ThermoFisher, UK), measured on a BMG CLARIOstar (BMG Labtech, UK). Cell homogenates (80 µg protein) were separated by a 10% sodium dodecyl sulfate-polyacrylamide gel (SDS-PAGE) and transferred to a nitrocellulose membrane. After blots had been washed with TBST (10 mM Tris, 150 mM NaCl, 0.05% Tween-20; pH 7.6) the membrane was blocked with 5% skimmed milk powder in TBST for 1 hour and incubated overnight at 4 °C with a purified mouse monoclonal antibody against human HIF-1α (BD Biosciences, UK), HIF-2α (Santa Cruz, USA) or a rabbit monoclonal antibody against β-actin (Sigma-Aldrich, UK) at dilutions recommended by the manufacturers. The membranes were washed and then incubated for 1 hour with the required secondary IgG horseradish peroxidase labelled antibody (goat anti-mouse or goat anti-rabbit). Detection was performed using West Femto chemiluminescence detection reagent (Pierce and Warner Ltd, UK) and exposed to photographic film (Amersham™ Hyperfilm, GE Healthcare) in a dark room. Films were developed using Kodak™ -D19 developer and fixer (Sigma-Aldrich).

2.8 Electron microscopy

Scanning electron microscopy (EM) images were generated to confirm EV release under normoxic and hypoxic (1% O_2) conditions. HECVs were washed in PBS and fixed in glutaraldehyde (Sigma-Aldrich, UK) in Sorensen's phosphate buffer (1% v/v) at room temperature for 1 hour. Samples were then dehydrated through graded isopropanol at 50, 70, 90 and 100% for 10 minutes each, followed by three exchanges in hexamethyldisilazane (Sigma-Aldrich, UK). Samples were then air dried and splutter-coated with gold and viewed at 5kV using a JEOL 840A scanning electron microscope (JEOL Tokyo, Japan).

Isolated EVs were visualised using transmission EM. Isolated EVs in PBS were negatively stained by placing carbon-coated grids onto 50 µL droplet of reagent for 30 minutes. Vesicles were fixed in 1% glutaraldehyde in Sorensen's phosphate buffer (1:1 v/v) for 10 minutes at room temperature. Grids were then washed (3 x 1 min in PBS and 6 x 1 min in water) before negative staining with 2% (w/v) uranyl acetate for 10 min. Surplus staining was removed from grids and allowed to air dry before EV samples were examined in a Philips CM12 TEM (FEI UK Ltd) at 80 kV.

2.9 Characterisation of EVs

Flow cytometry was used to assess the surface adhesion molecule profile of HECVs incubated at both normoxia and hypoxia, and their corresponding EVs. Antibodies used for cytometric analysis were obtained from Biolegend® (BioLegend, San Diego, CA, USA). They include; anti-CD62P [P-selectin], anti-CD51P [VCAM-1], anti-CD54 [ICAM-1], anti-CD562E [E-selectin], anti-CD31 [PECAM-1], and annexin V-FITC. Annexin V positivity was chosen to reflect the extent of phosphotidylserine (PS) exposure on the surface of EVs. All antibodies were allophycocyanin conjugated and mouse anti-human. Flow cytometry was performed using a BD Canto dual laser bench top flow cytometer, equipped with 488 nm and 633 nm lasers and BD FACS Diva software (v 5.0.3). Carboxylated polysterene beads (200, 500 and 1000 nm in diameter, (IZON, Oxford, UK)) were used to set the EV gate, and were distinguishable as three distinct populations. HECVs were analysed for forward scatter area and side scatter area whilst EVs were run on forward scatter area and side scatter area that were set to logarithmic scale. Acquisition was terminated upon recording 10,000 events, gated based on their forward scatter and side scatter characteristics. Fluorescence minus one (FMO) stains were used to set the positive gates for each antibody. Appendix Figure A3 shows a representative dot plot showing fluorescence-minus-one (A) and the EV gating strategy (B).

Time-resolved fluorescence was used to assess the surface protein and content of the isolated EVs derived from both normoxia and hypoxia, as described previously [44]. $1x10^9$ EVs were loaded onto a high protein binding 96-well plate (Greiner Bio-One, Germany) overnight at 4°C, before non-specific sites were blocked with 1% BSA (R&D Systems) for two hours. EVs were permeabilised using a RIPA lysis buffer (Santa Cruz, CA, USA) to allow analysis of intravesicular exosomal and endothelial markers. EVs were incubated overnight with mouse anti-human antibodies for the exosomal markers CD9, ALIX and TSG101, the endothelial marker CD144 (VE-Cadherin) and HIF-1α (Abcam, Cambridge, UK) overnight at 4°C. Markers were detected using a biotinylated anti-mouse igG secondary antibody (PerkinElmer, Buckinghamshire, UK) and a streptavidin:europium conjugate (PerkinElmer, Buckinghamshire, UK) and measured by time-resolved fluorescence (delay time: 400 µs, measurement window: 400 µs) using a BMG Labtech FLUOstar Optima.

2.10 Statistics

Data were analysed using GraphPad Prism (version 5.0; GraphPad Software Inc., San Diego, USA). D'Agostino's K-squared test was used to check data for normality. A 2way ANOVA with Bonferroni correction was used to compare size distribution differences between hypoxia and normoxia. A 1way ANOVA followed by either a Dunnett's post-test to compare all groups to the normoxic control, or a Tukey's test to compare all pairs of columns with each other. Results are expressed as mean ± SEM unless stated. A *p*-value of <0.05 was regarded as statistically significant.

3. Results

3.1 Effect of hypoxia on EV size, concentration and distribution

Hypoxia exposure (1%, 2% and 5% O_2) enhanced EV production in comparison to HECVs maintained at normoxia (1% O_2: 1766 ± 63.4 EVs/cell, 2% O_2: 1179 ± 59 EVs/cell, 5% O_2: 659 ± 48 EVs/cell vs 21% O_2: 133 ± 15 EVs/cell, Figure 1A, $p < 0.001$). However, 10% and 20% O_2 did not change EV production (10% O_2: 190.2 ± 40 EVs/cell, 20% O_2: 218 ± 57 EVs/cell $p>0.05$) compared to normoxia (Figure 1A). Hypoxic conditions did not affect EV mean size: 21% O_2: 134 ± 8 nm; 1% O_2: 131 ± 27 nm; 2% O_2: 133 ± 33 nm; 5% O_2: 143 ± 38 nm; 10% O_2: 133 ± 38 nm, 20% O_2: 132 ± 30 nm, $p> 0.05$. Western blot analysis revealed the presence of HIF-1α in cells exposed to 1-5% O_2 for 24 hours. HIF-1α was not detected in cells exposed to 10% or 20% O_2 (Figure 1B).

On assessment of EV size distribution (split by 50 nm bin size for analysis), cells exposed to 1% O_2 in particular had an elevated EV concentration within a diameter range of 51 – 350 nm (51 – 100 nm: 21% O_2; 16 ± 5 EVs/cell vs 1% O_2; 205 ± 44 EVs/ cell. 101 – 150 nm: 21% O_2; 33 ± 8 EVs/cell vs 1% O_2; 441 ± 66 EVs/cell. 151 – 200 nm: 21% O_2; 29 ± 5 EVs/cell vs 1% O_2; 401 ± 26 EVs/ cell. 201 – 250 nm: 21% O_2; 22 ± 4 EVs/cell vs 1% O_2; 300 ± 18 EVs/ cell. 251-300 nm: 21% O_2; 14 ± 3 EVs/cell vs 1% O_2; 210 ± 30 EVs/ cell. 301-350 nm: 1% O_2: 7 ± 2 EVs/cell vs 1% O_2: 132 ± 22 EVs/cell ($p < 0.001$ for all comparisons). EV distribution between 351 – 1 μm was similar between normoxic and hypoxic cells, $p > 0.05$ (Figure 2).

Cells incubated in normoxia exposed to the hypoxia mimetic agent desferrioxamine (100 μM) produced significantly higher EVs compared to cells exposed to normoxia alone (1212 ± 109 EVs/cell vs 133 ± 15.2 EVs/cell, $p < 0.001$). The addition of desferrioxamine to cells already exposed to hypoxia (1% O_2) had no influence on EV production compared to hypoxia exposure alone (1% O_2: 1673 ± 60 EVs/cell vs 1% O_2 DFO: 1733 ± 87 EVs/cell, $p > 0.05$) (Figure 3A). Chemically induced hypoxia by desferrioxamine was confirmed by Western blot detection of HIF-1α in cells incubated in normoxia. (Figure 3B).

3.2 Viability and apoptosis

Cells exposed to 1% O_2 had similar caspase 3/7 activity to control cells (688 ± 7 vs 612 ± 73, relative luminescence units (RLU) $p > 0.05$). No difference was found in cell viability for cells exposed to 1% O_2 compared to control cells assessed either by the MTS cell proliferation assay (1% O_2: 1.99 ± 0.04 vs normoxia: 1.73 ± 0.24, absorbance [AU], $p > 0.05$), or by trypan blue exclusion (1% O_2: 87 ± 1% vs normoxia: 89 ± 1%, $p > 0.05$)

3.3 Morphology of HECV and HECV-derived-EVs.

Scanning electron microscopy confirmed the release of EVs from HECVs. Cells were homogenous and approximately 10-15 μm in diameter. Appendix Figure A4A shows HECVs incubated in normoxic (21% O_2) conditions. Cells appear relatively dormant and have distinct cell boundaries. Appendix Figure A4B shows HECV cells incubated in hypoxic conditions (1% O_2) for 24 hours. These cells appear rounded, producing a higher number of vesicles compared to the normoxic cells. Transmission electron microscopy confirmed the presence of EVs isolated from HECVs incubated in normoxia (Appendix Figure A4C) and hypoxia (Appendix Figure A4D). These EVs appear granular and approximately 100-250 nm in diameter.

3.4 Characterisation of EVs

Flow cytometry confirmed the presence of VCAM-1, ICAM-1, PECAM-1, P-selectin and E-selectin on HECVs which did not alter after hypoxia exposure ($p > 0.05$, Appendix Figure A5A). The presence of these adhesion molecules was reflected in the EVs. However these also did not change as a function of hypoxia exposure ($p > 0.05$, Appendix Figure A5B). There were no differences in the proportion of annexin V positive EVs between hypoxia-derived EVs (11 ± 0.2%) and normoxia-derived EVs (11 ± 0.25%, $p > 0.05$).

Time-resolved fluorescence revealed no difference between the level of the exosomal markers CD9, TSG101 or ALIX and the endothelial marker VE-Cadherin in EVs isolated from normoxia and hypoxia (CD9: 21% O_2; 37651± 1724 vs 1% O_2; 39528 ± 2507. TSG101: 21% O_2; 14495 ± 549 vs 1% O_2; 15979 ± 1953. ALIX: 21% O_2; 8683 ± 818 vs 1% O_2; 10310 ± 510. CD144: 21% O_2; 2182 ± 178 vs 1% O_2; 2601 ± 234, arbitrary units, $p > 0.05$) (Figure 2). HIF-1α was present in EVs isolated from hypoxic HECVs and absent in those isolated from normoxia (21% O_2; 115 ± 25 vs 1% O_2; 10310 ± 520, $p < 0.001$) (Appendix Figure A6).

3.5 Effect of silencing HIF-1α and HIF-2α

To confirm the role of HIF-1α and/or HIF-2α in the hypoxic enhancement of EV release, HECVs were transfected with a siRNA targeting either HIF-1α, or HIF-2α. Cells transfected with HIF-1α siRNA failed to show an enhancement in EV release following hypoxia compared to cells transfected with control siRNA or cells exposed to hypoxia alone (HIF-1α siRNA in 1% O_2: 243 ± 20 EVs/cell, control siRNA in 1% O_2: 1680 ± 473 EVs/cell, 1% O_2:1680 ± 250 EVs/cell, $p < 0.001$) (Figure 4A). EV production in cells transfected with HIF-1α siRNA in hypoxia was similar to that of the normoxia control (158 ± 38 EVs/cell, $p > 0.05$). HECVs were also transfected with HIF-2α siRNA. Unlike HIF-1α siRNA transfection, HIF-2α silencing had no effect on EV production compared to cells transfected with control siRNA or exposed to hypoxia alone (HIF-2α siRNA in 1% O_2: 1549 ± 46 EVs/cell, control siRNA in 1% O_2: 1608 ± 69 EVs/cell, 1% O_2:1774 ± 132 EVs/cell, $p < 0.05$.

Western blotting confirmed that cells transfected with HIF-1α and HIF-2α siRNA successfully inhibited gene expression, whilst the control siRNA had no impact on HIF-1α/-2α expression (Figure 4C, 4D).

3.6 Effect of sodium nitrite on EV production

To assess the effect of NO on the hypoxia-mediated enhancement of EV production, HECVs were treated with $NaNO_2$. There was little evidence to suggest that $NaNO_2$ had any effect on EV production at 21% O_2, (21% O_2:132 ± 15 EVs/cell vs 21% O_2 + $NaNO_2$: 125 ± 19 EVs/cell, p >0.05). However, $NaNO_2$ significantly reduced the hypoxic enhancement of EV production (1% O_2: 1859 ± 67 EVs/cell vs. 1% O_2 + $NaNO_2$: 905 ± 78 EVs/cell, p <0.001). Treatment of HECVs in hypoxia with allopurinol in addition to $NaNO_2$ attenuated the $NaNO_2$-induced suppression of hypoxia-mediated EV release, (1% O_2 + $NaNO_2$; 905 ± 78 EVs/cell vs 1% O_2, $NaNO_2$ + Allopurinol; 1414 ± 141 EVs/cell, p <0.001). Allopurinol alone had no effect on EV production in hypoxia (1824 ± 69 EVs/cell, p > 0.05 (Figure 4B). The NO donor S-Nitrosoglutathione (GSNO) also significantly reduced EV production in hypoxia (896 ± 27 EVs/cell, p < 0.001) (Figure 5A). Western blots confirmed that $NaNO_2$ addition in hypoxia reduced the expression of HIF-1α. The addition of allopurinol in the presence of $NaNO_2$ appeared to restore HIF-1α expression in HECVs (Figure 5B).

3.7 Effect of hypoxia and sodium nitrite on EV production in HUVECs

In order to validate our findings in the HECV cell line, the effect of hypoxia and sodium nitrite on EV production was also assessed in HUVECs. $NaNO_2$ had no effect on EV production in normoxia (21% O_2: 43 ± 5.6 EVs/cell vs 21% O_2 + $NaNO_2$: 41 ± 4 EVs/cell, p > 0.05). Hypoxia greatly enhanced EV production compared to normoxia (1% O_2: 291 ± 23 EVs/cell vs 21% O_2: 43 ± 6 EVs/cell, p < 0.001). Furthermore, the addition of $NaNO_2$ significantly reduced EV production in hypoxia (1% O_2 + $NaNO_2$: 153 ± 11 EVs/cell vs 1% O_2: 291 ± 23 EVs/cell, p < 0.001) (Figure 6A). Western blots confirmed that $NaNO_2$ addition in hypoxia reduced the expression of HIF-1α (Figure 6B).

4. Discussion

Our study shows that hypoxia-induced enhancement in EV production is mediated by HIF-1α in endothelial cells. We extend these observations to show that NO_2^- alleviates EV production selectively during hypoxia at least in part by reduction to NO via xanthine oxidoreductase, in turn favouring the oxygen sensitive degradation of HIF-1α and subsequent suppression of HIF-mediated EV release.

During pathological conditions cellular O_2 levels can often be insufficient to meet physiological demands. The resulting hypoxia is an important feature of cardiovascular disease, sleep apnoea, and cancer and is associated with poor patient outcomes [45]. Endothelial cells exposed to hypoxia for 24 hours demonstrated enhanced EV production at 5% O_2 and lower. This is in accordance with previous studies which have demonstrated that hypoxia is associated with increased endothelial-derived EV production *in vivo* [16,17]. Arterial blood pO_2 is normally within the range 10-14% O_2 (75-100 mmHg), with venous levels approximately 4-5.5% O_2 (30-40 mmHg). At an arterial O_2 of 8% (60 mmHg) there is a steep decline in oxygen saturation, and a human would require supplemental breathing, whereas <4% O_2 (26 mmHg) can be considered extreme hypoxia [46]. Given these reference ranges, we rationalised 5% O_2 in our studies represents an accurate model of a hypoxic condition for cells in culture, whereas less than 1% O_2 reflects severe hypoxia.

Endothelial EV signalling has been shown to enhance activation and adhesion of platelets, leading to the formation of a thrombus [47]. Studies have shown that increased EV release by activated endothelial cells was associated with cardiovascular events in patients with stroke history [48]. It remains unclear whether the pathological effects of these vesicles are due to differences in biological cargo compared to vesicles released under resting conditions, or simply due to an increased number of vesicles being produced. In our studies, we failed to measure a difference in numerous adhesion molecules between vesicles released from cells in hypoxia compared to cells in normoxia. Interestingly, we found HIF-1α was present in our EV sample, and was elevated under hypoxic conditions, potentially allowing for paracrine signalling to nearby cells. Previous studies have shown that nuclear translocation is not required for HIF-1α stabilization after its translation in the cytoplasm [49], and thus may be packaged into EV during their formation via the classical pathway of exosome formation. This pathway is governed by the endosomal sorting complex required for transport (ESCRT), which orchestrates the formation of intraluminal vesicles within multivesicular bodies following invagination of the cells plasma membrane [50]. Notably, we were unable to detect HIF-1α in EVs derived from HIF-1α siRNA treated cells.

Consistent with previous reports in breast cancer cell lines [51] we provide evidence that HIF-1α is pivotal in the hypoxia-induced enhancement of EV release in endothelial cells. In contrast, HIF-2α had no influence on hypoxic EV production. Thus, hypoxia-mediated EV production may utilise

common cellular pathways regardless of the cell type. HIF-1α is thought to be involved in acute hypoxia (2-24 hours), with HIF-2α involved in cellular adaptation to chronic hypoxia (>24 hours) [52,53]. A third HIF isoform, HIF-3α, also regulates the cellular response to hypoxia but was not studied here. HIF-3α lacks the transactivation domain found in both HIF-1α and HIF-2α isoforms, and is said to be a negative regulator of HIF-1α and HIF-2α induced gene expression [54].

Acute hypoxia has been shown to increase calcium to levels similar to those observed during agonist stimulation of endothelial cells, but too low to cause apoptosis or a reduction in viability [55]. The mechanism of EV release by cells is still not fully characterised, although it is known to be dependent on a rise in cytosolic calcium, and subsequent activation of calpain and protein kinases, allowing cytoskeletal remodelling, translocation of phosphotidylserine, and enhanced permeability to potassium with associated osmotic effects [56–60]. Indeed, HIF-1α activation has recently been shown to permit cytoskeleton reorganization in endothelial cells [61]. Furthermore, RAB22A has previously been identified as a potential mediator of HIF-1α induced EV release. RAB22A is a small GTPase involved in trafficking between endosomal compartments, which is localised to budding EVs [62]. A study by Wang *et al* showed expression of this GTPase was HIF-1α mediated, with RAB22A knockdown completely eliminating the increase in EV production in hypoxia [63].

Moreover, HIF has previously been shown to induce autophagy, via upregulation of the BNIP-3 gene, promoting the BNIP-3/Beclin pathway [64]. Additionally, HIF-1α is an inhibitor of the mammalian target of rapamycin (mTOR), via upregulation of the target genes REDD1 and REDD2 [65]. mTOR is a key regulator of autophagy induction, with activated mTOR supressing autophagy, and negative regulation of mTOR promoting it [66]. Autophagy and exosome release are coordinated mechanisms that share common cellular machinery [67], with some studies showing that induction of autophagy enhances EV release [68]. Indeed, the p38 mitogen-activated protein kinase (MAPK) that is involved in autophagy has also been shown to enhance procoagulant endothelial EV release [56]. This pathway could therefore explain the increase in EV generation seen in this study.

To our knowledge this is the first study to demonstrate that NO alleviates the hypoxic enhancement of EV production in endothelial cells, through the hypoxia-selective reduction of NO_2^- to NO via xanthine oxidoreductase. This reduction was observed in both an endothelial cell line (HECVs) and primary endothelial cells (HUVECs). This observation is supported by previous work which showed impaired NO production induces endothelial EV production *in vitro* [32]. In contrast to the constitutively expressed β-subunit of HIF, HIF-1α is an oxygen-regulated subunit. Numerous factors have been shown to modulate HIF-1α activation and stabilisation in general, including NO [69]. NO_2^- represents a bioactive "storage pool" for NO under certain conditions, such as hypoxia. This pathway, dubbed the "nitrate-nitrite-nitric oxide pathway", has been said to complement the L-arginine-eNOS

pathway perfectly, ensuring NO production continues during conditions where oxygen-dependent eNOS activity is compromised. Indeed we, and others, have previously shown that NO_2^- administered intravenously can protect against vascular reperfusion injury [70,71].

The regulation of HIF-1α by NO in hypoxia involves the mitochondrial cytochrome c oxidase (CcO), which plays a central role in oxidative phosphorylation and ATP synthesis. NO can readily modulate the activity of CcO and therefore its O_2 consumption. In hypoxia, competitive binding of NO inhibits CcO allowing the redistribution of intracellular O_2, leading to increased O_2 availability for prolyl hydroxylation and subsequent degradation of HIF-1α, which has been shown by numerous studies [30,31,69]. Collectively, our data suggest that although HIF-1 appears to be the master hypoxic regulator which governs hypoxia-induced EV release, under hypoxic conditions NO_2^- is metabolised to NO, promoting the degradation of HIF-1α and subsequent suppression of EV release. Interestingly, HIF-1α can enhance NO production via upregulation of inducible nitric oxide synthase (iNOS), highlighting a potential negative feedback mechanism [72,73].

Treatment of endothelial cells with allopurinol, in the presence of $NaNO_2$, largely inhibited the NO_2-attributed suppression of EV production. This confirms that under hypoxic conditions, xanthine oxidoreductase plays an important role in the reduction of NO_2^- to NO. However, the presence of allopurinol failed to completely restore EV production seen in hypoxia alone, and it is therefore likely that multiple mechanisms, including mitochondrial reduction and aldehyde dehydrogenase play a role in reducing NO_2^- to NO in endothelial cells [74].

In summary, this study suggests a novel means by which inorganic nitrite (NO_2^-) alleviates the hypoxic enhancement in EV production. Future studies should further elucidate which downstream targets of HIF-1α may be responsible for the increase in EV production, and investigate whether enhancing NO bioavailability affects EV levels in clinical models of ischaemia.

Acknowledgements

The authors would like to thank Dr Christopher Von Ruhland for his assistance with the electron microscopy.

Sources of Funding

This work was funded by a Health and Care Research Wales Scholarship (N.B.H), the Mrs. John Nixon Scholarship (G.R.W) and the Cardiac Research Development Fund (G.R.W).

References

[1] E. van der Pol, A.N. Böing, P. Harrison, A. Sturk, R. Nieuwland, Classification, functions, and clinical relevance of extracellular vesicles., Pharmacol. Rev. 64 (2012) 676–705. doi:10.1124/pr.112.005983.

[2] B. György, T.G. Szabó, M. Pásztói, Z. Pál, P. Misják, B. Aradi, et al., Membrane vesicles, current state-of-the-art: Emerging role of extracellular vesicles, Cell. Mol. Life Sci. 68 (2011) 2667–2688. doi:10.1007/s00018-011-0689-3.

[3] M.E. Tushuizen, M. Diamant, A. Sturk, R. Nieuwland, Cell-derived microparticles in the pathogenesis of cardiovascular disease: friend or foe?, Arterioscler. Thromb. Vasc. Biol. 31 (2011) 4–9. doi:10.1161/ATVBAHA.109.200998.

[4] F. Wendler, R. Favicchio, T. Simon, C. Alifrangis, J. Stebbing, G. Giamas, Extracellular vesicles swarm the cancer microenvironment: from tumor–stroma communication to drug intervention, Oncogene. (2016). doi:10.1038/onc.2016.253.

[5] C. D'Souza-Schorey, J.W. Clancy, Tumor-derived microvesicles: shedding light on novel microenvironment modulators and prospective cancer biomarkers., Genes Dev. 26 (2012) 1287–99. doi:10.1101/gad.192351.112.

[6] N. Yamada, Y. Kuranaga, M. Kumazaki, H. Shinohara, K. Taniguchi, Y. Akao, et al., Colorectal cancer cell-derived extracellular vesicles induce phenotypic alteration of T cells into tumor-growth supporting cells with transforming growth factor-β1-mediated suppression, Oncotarget. 7 (2016) 27033–27043.

[7] S.A. Bellingham, B.B. Guo, B.M. Coleman, A.F. Hill, Exosomes: Vehicles for the Transfer of Toxic Proteins Associated with Neurodegenerative Diseases?, Front. Physiol. 3 (2012) 124. doi:10.3389/fphys.2012.00124.

[8] A. Schneider, M. Simons, Exosomes: vesicular carriers for intercellular communication in neurodegenerative disorders, Cell Tissue Res. 352 (2013) 33–47. doi:10.1007/s00441-012-1428-2.

[9] L.J. Vella, R.A. Sharples, R.M. Nisbet, R. Cappai, A.F. Hill, The role of exosomes in the processing of proteins associated with neurodegenerative diseases, Eur. Biophys. J. 37 (2008) 323–332. doi:10.1007/s00249-007-0246-z.

[10] A.G. Thompson, E. Gray, S.M. Heman-Ackah, I. Mäger, K. Talbot, S. El Andaloussi, et al., Extracellular vesicles in neurodegenerative disease - pathogenesis to biomarkers., Nat. Rev. Neurol. 12 (2016) 346–57. doi:10.1038/nrneurol.2016.68.

[11] L.L. Horstman, W. Jy, J.J. Jimenez, Y.S. Ahn, Endothelial microparticles as markers of endothelial dysfunction., Front. Biosci. 9 (2004) 1118–35.

[12] A. Gaceb, M.C. Martinez, R. Andriantsitohaina, Extracellular vesicles: new players in cardiovascular diseases., Int. J. Biochem. Cell Biol. 50 (2014) 24–8. doi:10.1016/j.biocel.2014.01.018.

[13] M.J. Vanwijk, E. Vanbavel, a Sturk, R. Nieuwland, M icroparticles in cardiovascular diseases, Cardiovasc. Res. 59 (2003) 277–287.

[14] P.-E. Rautou, A.-C. Vion, N. Amabile, G. Chironi, A. Simon, A. Tedgui, et al., Microparticles, vascular function, and atherothrombosis., Circ. Res. 109 (2011) 593–606. doi:10.1161/CIRCRESAHA.110.233163.

[15] C.M. Boulanger, A. Scoazec, T. Ebrahimian, P. Henry, E. Mathieu, A. Tedgui, et al., Circulating microparticles from patients with myocardial infarction cause endothelial dysfunction., Circulation. 104 (2001) 2649–2652. doi:10.1161/hc4701.100516.

[16] R. V Vince, B. Chrismas, A.W. Midgley, L.R. McNaughton, L.A. Madden, Hypoxia mediated release of endothelial microparticles and increased association of S100A12 with circulating

476 neutrophils., Oxid. Med. Cell. Longev. 2 (2009) 2–6.

477 [17] M. Lichtenauer, B. Goebel, M. Fritzenwanger, M. Förster, S. Betge, A. Lauten, et al.,
478 Simulated temporary hypoxia triggers the release of CD31+/Annexin+ endothelial
479 microparticles: A prospective pilot study in humans., Clin. Hemorheol. Microcirc. (2014).
480 doi:10.3233/CH-141908.

481 [18] P. Vaupel, A. Mayer, Hypoxia in cancer: significance and impact on clinical outcome., Cancer
482 Metastasis Rev. 26 (2007) 225–39. doi:10.1007/s10555-007-9055-1.

483 [19] C. Peers, M.L. Dallas, H.E. Boycott, J.L. Scragg, H.A. Pearson, J.P. Boyle, Hypoxia and
484 neurodegeneration., Ann. N. Y. Acad. Sci. 1177 (2009) 169–77. doi:10.1111/j.1749-
485 6632.2009.05026.x.

486 [20] G.L. Semenza, Hypoxia-inducible factor 1: oxygen homeostasis and disease pathophysiology.,
487 Trends Mol. Med. 7 (2001) 345–50.

488 [21] O.G. de Jong, M.C. Verhaar, Y. Chen, P. Vader, H. Gremmels, G. Posthuma, et al., Cellular
489 stress conditions are reflected in the protein and RNA content of endothelial cell-derived
490 exosomes., J. Extracell. Vesicles. 1 (2012). doi:10.3402/jev.v1i0.18396.

491 [22] G.L. Semenza, HIF-1 mediates metabolic responses to intratumoral hypoxia and oncogenic
492 mutations., J. Clin. Invest. 123 (2013) 3664–71. doi:10.1172/JCI67230.

493 [23] C.M. Lambert, M. Roy, G.A. Robitaille, D.E. Richard, S. Bonnet, HIF-1 inhibition decreases
494 systemic vascular remodelling diseases by promoting apoptosis through a hexokinase 2-
495 dependent mechanism., Cardiovasc. Res. 88 (2010) 196–204. doi:10.1093/cvr/cvq152.

496 [24] H. Tian, S.L. McKnight, D.W. Russell, Endothelial PAS domain protein 1 (EPAS1), a
497 transcription factor selectively expressed in endothelial cells., Genes Dev. 11 (1997) 72–82.

498 [25] I.P. Stolze, D.R. Mole, P.J. Ratcliffe, Regulation of HIF: prolyl hydroxylases., Novartis Found.
499 Symp. 272 (2006) 15-25-36.

500 [26] C.P. Bracken, A.O. Fedele, S. Linke, W. Balrak, K. Lisy, M.L. Whitelaw, et al., Cell-specific
501 Regulation of Hypoxia-inducible Factor (HIF)-1␣ and HIF-2␣ Stabilization and
502 Transactivation in a Graded Oxygen Environment *, (2006). doi:10.1074/jbc.M600288200.

503 [27] L. Østergaard, U. Simonsen, Y. Eskildsen-Helmond, H. Vorum, N. Uldbjerg, B. Honoré, et al.,
504 Proteomics reveals lowering oxygen alters cytoskeletal and endoplasmatic stress proteins in
505 human endothelial cells, Proteomics. 9 (2009) 4457–4467. doi:10.1002/pmic.200800130.

506 [28] L.E. Campbell, J. Nelson, E. Gibbons, A.M. Judd, J.D. Bell, Membrane Properties Involved in
507 Calcium-Stimulated Microparticle Release from the Plasma Membranes of S49 Lymphoma
508 Cells, Sci. World J. 2014 (2014) 1–7. doi:10.1155/2014/537192.

509 [29] K.M. Naseem, The role of nitric oxide in cardiovascular diseases., Mol. Aspects Med. 26
510 (2005) 33–65. doi:10.1016/j.mam.2004.09.003.

511 [30] T. Hagen, C.T. Taylor, F. Lam, S. Moncada, Redistribution of intracellular oxygen in hypoxia
512 by nitric oxide: effect on HIF1alpha., Science. 302 (2003) 1975–8.
513 doi:10.1126/science.1088805.

514 [31] E. Metzen, J. Zhou, W. Jelkmann, J. Fandrey, B. Brüne, Nitric oxide impairs normoxic
515 degradation of HIF-1alpha by inhibition of prolyl hydroxylases., Mol. Biol. Cell. 14 (2003)
516 3470–81. doi:10.1091/mbc.E02-12-0791.

517 [32] J.-M. Wang, Y. Wang, J.-Y. Huang, Z. Yang, L. Chen, L.-C. Wang, et al., C-Reactive protein-
518 induced endothelial microparticle generation in HUVECs is related to BH4-dependent NO
519 formation., J. Vasc. Res. 44 (2007) 241–8. doi:10.1159/000100558.

520 [33] J.O. Lundberg, E. Weitzberg, M.T. Gladwin, The nitrate-nitrite-nitric oxide pathway in
521 physiology and therapeutics., Nat. Rev. Drug Discov. 7 (2008) 156–67. doi:10.1038/nrd2466.

522 [34] P.E. James, G.R. Willis, J.D. Allen, P.G. Winyard, A.M. Jones, Nitrate pharmacokinetics:

Taking note of the difference., Nitric Oxide. 48 (2015) 44–50. doi:10.1016/j.niox.2015.04.006.

[35] R.S. Khambata, S.M. Ghosh, A. Ahluwalia, "Repurposing" of Xanthine Oxidoreductase as a Nitrite Reductase: A New Paradigm for Therapeutic Targeting in Hypertension., Antioxid. Redox Signal. 23 (2015) 340–53. doi:10.1089/ars.2015.6254.

[36] H. Li, A. Samouilov, X. Liu, J.L. Zweier, Characterization of the magnitude and kinetics of xanthine oxidase-catalyzed nitrate reduction: evaluation of its role in nitrite and nitric oxide generation in anoxic tissues., Biochemistry. 42 (2003) 1150–9. doi:10.1021/bi026385a.

[37] K. Cosby, K.S. Partovi, J.H. Crawford, R.P. Patel, C.D. Reiter, S. Martyr, et al., Nitrite reduction to nitric oxide by deoxyhemoglobin vasodilates the human circulation., Nat. Med. 9 (2003) 1498–505. doi:10.1038/nm954.

[38] S. Shiva, Z. Huang, R. Grubina, J. Sun, L.A. Ringwood, P.H. MacArthur, et al., Deoxymyoglobin is a nitrite reductase that generates nitric oxide and regulates mitochondrial respiration, Circ. Res. 100 (2007) 654–661. doi:10.1161/01.RES.0000260171.52224.6b.

[39] S. Basu, N.A. Azarova, M.D. Font, S.B. King, N. Hogg, M.T. Gladwin, et al., Nitrite reductase activity of cytochrome c., J. Biol. Chem. 283 (2008) 32590–7. doi:10.1074/jbc.M806934200.

[40] P.R. Castello, P.S. David, T. McClure, Z. Crook, R.O. Poyton, Mitochondrial cytochrome oxidase produces nitric oxide under hypoxic conditions: implications for oxygen sensing and hypoxic signaling in eukaryotes., Cell Metab. 3 (2006) 277–87. doi:10.1016/j.cmet.2006.02.011.

[41] B. Baudin, A. Bruneel, N. Bosselut, M. Vaubourdolle, A protocol for isolation and culture of human umbilical vein endothelial cells., Nat. Protoc. 2 (2007) 481–5. doi:10.1038/nprot.2007.54.

[42] J. Webber, A. Clayton, How pure are your vesicles?, J. Extracell. Vesicles. 2 (2013).

[43] G.R. Willis, K. Connolly, K. Ladell, T.S. Davies, I.A. Guschina, D. Ramji, et al., Young women with polycystic ovary syndrome have raised levels of circulating annexin V-positive platelet microparticles., Hum. Reprod. 29 (2014) 2756–63. doi:10.1093/humrep/deu281.

[44] K.D. Connolly, I.A. Guschina, V. Yeung, A. Clayton, M.S. Draman, C. Von Ruhland, et al., Characterisation of adipocyte-derived extracellular vesicles released pre- and post-adipogenesis., J. Extracell. Vesicles. 4 (2015) 29159.

[45] G.L. Semenza, Oxygen sensing, hypoxia-inducible factors, and disease pathophysiology., Annu. Rev. Pathol. 9 (2014) 47–71. doi:10.1146/annurev-pathol-012513-104720.

[46] J.-A. Collins, A. Rudenski, J. Gibson, L. Howard, R. O'Driscoll, Relating oxygen partial pressure, saturation and content: the haemoglobin-oxygen dissociation curve., Breathe (Sheffield, England). 11 (2015) 194–201. doi:10.1183/20734735.001415.

[47] P. Cherian, G.J. Hankey, J.W. Eikelboom, J. Thom, R.I. Baker, A. McQuillan, et al., Endothelial and platelet activation in acute ischemic stroke and its etiological subtypes., Stroke. 34 (2003) 2132–7. doi:10.1161/01.STR.0000086466.32421.F4.

[48] S.-T. Lee, K. Chu, K.-H. Jung, J.-M. Kim, H.-J. Moon, J.-J. Bahn, et al., Circulating CD62E+ microparticles and cardiovascular outcomes., PLoS One. 7 (2012) e35713. doi:10.1371/journal.pone.0035713.

[49] E. Berra, D. Roux, D.E. Richard, J. Pouysségur, Hypoxia-inducible factor-1 alpha (HIF-1 alpha) escapes O(2)-driven proteasomal degradation irrespective of its subcellular localization: nucleus or cytoplasm., EMBO Rep. 2 (2001) 615–20. doi:10.1093/embo-reports/kve130.

[50] M. Colombo, G. Raposo, C. Théry, Biogenesis, Secretion, and Intercellular Interactions of Exosomes and Other Extracellular Vesicles, Annu. Rev. Cell Dev. Biol. 30 (2014) 255–289. doi:10.1146/annurev-cellbio-101512-122326.

[51] H.W. King, M.Z. Michael, J.M. Gleadle, Hypoxic enhancement of exosome release by breast

570 cancer cells., BMC Cancer. 12 (2012) 421. doi:10.1186/1471-2407-12-421.
571 [52] Q. Lin, X. Cong, Z. Yun, A. Harris, E. Rankin, A. Giaccia, et al., Differential hypoxic
572 regulation of hypoxia-inducible factors 1alpha and 2alpha., Mol. Cancer Res. 9 (2011) 757–65.
573 doi:10.1158/1541-7786.MCR-11-0053.
574 [53] M.Y. Koh, G. Powis, Passing the baton: the HIF switch., Trends Biochem. Sci. 37 (2012) 364–
575 72. doi:10.1016/j.tibs.2012.06.004.
576 [54] P. Zhang, Q. Yao, L. Lu, Y. Li, P.-J. Chen, C. Duan, Hypoxia-inducible factor 3 is an oxygen-
577 dependent transcription activator and regulates a distinct transcriptional response to hypoxia.,
578 Cell Rep. 6 (2014) 1110–21. doi:10.1016/j.celrep.2014.02.011.
579 [55] T. Arnould, C. Michiels, I. Alexandre, J. Remacle, Effect of hypoxia upon intracellular
580 calcium concentration of human endothelial cells., J. Cell. Physiol. 152 (1992) 215–21.
581 doi:10.1002/jcp.1041520127.
582 [56] A.M. Curtis, P.F. Wilkinson, M. Gui, T.L. Gales, E. Hu, J.M. Edelberg, p38 mitogen-activated
583 protein kinase targets the production of proinflammatory endothelial microparticles., J.
584 Thromb. Haemost. 7 (2009) 701–9. doi:10.1111/j.1538-7836.2009.03304.x.
585 [57] S. Cauwenberghs, M.A.H. Feijge, A.G.S. Harper, S.O. Sage, J. Curvers, J.W.M. Heemskerk,
586 Shedding of procoagulant microparticles from unstimulated platelets by integrin-mediated
587 destabilization of actin cytoskeleton., FEBS Lett. 580 (2006) 5313–20.
588 doi:10.1016/j.febslet.2006.08.082.
589 [58] P. Comfurius, J.M. Senden, R.H. Tilly, A.J. Schroit, E.M. Bevers, R.F. Zwaal, Loss of
590 membrane phospholipid asymmetry in platelets and red cells may be associated with calcium-
591 induced shedding of plasma membrane and inhibition of aminophospholipid translocase.,
592 Biochim. Biophys. Acta. 1026 (1990) 153–60.
593 [59] E. Reichstein, A. Rothstein, Effects of quinine on Ca++-induced K+ efflux from human red
594 blood cells., J. Membr. Biol. 59 (1981) 57–63.
595 [60] D. Allan, P. Thomas, Ca2+-induced biochemical changes in human erythrocytes and their
596 relation to microvesiculation., Biochem. J. 198 (1981) 433–40.
597 [61] A. Weidemann, J. Breyer, M. Rehm, K.-U. Eckardt, C. Daniel, I. Cicha, et al., HIF-1α
598 activation results in actin cytoskeleton reorganization and modulation of Rac-1 signaling in
599 endothelial cells, Cell Commun. Signal. 11 (2013) 80. doi:10.1186/1478-811X-11-80.
600 [62] J.G. Magadán, M.A. Barbieri, R. Mesa, P.D. Stahl, L.S. Mayorga, Rab22a regulates the sorting
601 of transferrin to recycling endosomes., Mol. Cell. Biol. 26 (2006) 2595–614.
602 doi:10.1128/MCB.26.7.2595-2614.2006.
603 [63] T. Wang, D.M. Gilkes, N. Takano, L. Xiang, W. Luo, C.J. Bishop, et al., Hypoxia-inducible
604 factors and RAB22A mediate formation of microvesicles that stimulate breast cancer invasion
605 and metastasis., Proc. Natl. Acad. Sci. U. S. A. 111 (2014) E3234-42.
606 doi:10.1073/pnas.1410041111.
607 [64] G. Bellot, R. Garcia-Medina, P. Gounon, J. Chiche, D. Roux, J. Pouysségur, et al., Hypoxia-
608 induced autophagy is mediated through hypoxia-inducible factor induction of BNIP3 and
609 BNIP3L via their BH3 domains., Mol. Cell. Biol. 29 (2009) 2570–81.
610 doi:10.1128/MCB.00166-09.
611 [65] J. Brugarolas, K. Lei, R.L. Hurley, B.D. Manning, J.H. Reiling, E. Hafen, et al., Regulation of
612 mTOR function in response to hypoxia by REDD1 and the TSC1/TSC2 tumor suppressor
613 complex., Genes Dev. 18 (2004) 2893–904. doi:10.1101/gad.1256804.
614 [66] C.H. Jung, S.-H. Ro, J. Cao, N.M. Otto, D.-H. Kim, mTOR regulation of autophagy., FEBS
615 Lett. 584 (2010) 1287–95. doi:10.1016/j.febslet.2010.01.017.
616 [67] F. Baixauli, C. LÃ³pez-OtÃ-n, M. Mittelbrunn, Exosomes and Autophagy: Coordinated
617 Mechanisms for the Maintenance of Cellular Fitness, Front. Immunol. 5 (2014) 403.

doi:10.3389/fimmu.2014.00403.

[68] C.M. Fader, D. Sánchez, M. Furlán, M.I. Colombo, Induction of autophagy promotes fusion of multivesicular bodies with autophagic vacuoles in k562 cells., Traffic. 9 (2008) 230–50. doi:10.1111/j.1600-0854.2007.00677.x.

[69] U. Berchner-Pfannschmidt, H. Yamac, B. Trinidad, J. Fandrey, Nitric oxide modulates oxygen sensing by hypoxia-inducible factor 1-dependent induction of prolyl hydroxylase 2., J. Biol. Chem. 282 (2007) 1788–96. doi:10.1074/jbc.M607065200.

[70] A. Webb, R. Bond, P. McLean, R. Uppal, N. Benjamin, A. Ahluwalia, Reduction of nitrite to nitric oxide during ischemia protects against myocardial ischemia-reperfusion damage, Proc. Natl. Acad. Sci. 101 (2004) 13683–13688. doi:10.1073/pnas.0402927101.

[71] T.E. Ingram, A.G. Fraser, R.A. Bleasdale, E.A. Ellins, A.D. Margulescu, J.P. Halcox, et al., Low-dose sodium nitrite attenuates myocardial ischemia and vascular ischemia-reperfusion injury in human models., J. Am. Coll. Cardiol. 61 (2013) 2534–41. doi:10.1016/j.jacc.2013.03.050.

[72] F. Jung, L.A. Palmer, N. Zhou, R.A. Johns, Hypoxic regulation of inducible nitric oxide synthase via hypoxia inducible factor-1 in cardiac myocytes., Circ. Res. 86 (2000) 319–25.

[73] R. Hu, A. Dai, S. Tan, Hypoxia-inducible factor 1 alpha upregulates the expression of inducible nitric oxide synthase gene in pulmonary arteries of hyposic rat., Chin. Med. J. (Engl). 115 (2002) 1833–7.

[74] S. Shiva, Nitrite: A Physiological Store of Nitric Oxide and Modulator of Mitochondrial Function., Redox Biol. 1 (2013) 40–44. doi:10.1016/j.redox.2012.11.005.

640 **Figures**

641 **Figure 1. The effect of hypoxia on EV concentration.** (A) EVs produced per cell at varying O_2
642 concentrations. (B) Western blot showing the presence and absence of HIF-1α at varying O_2
643 concentrations. Lane 1: 21% O_2. Lane 2: 1% O_2. Lane 3: 2% O_2. Lane 4: 5% O_2. Lane 5: 10% O_2. Lane
644 6: 20% O_2. Results represent [n = 5]. Each sample was analysed in quintuplicate and the mean was
645 used in further analysis. Data are expressed as mean ± SEM. *** reflects $p < 0.001$.

646

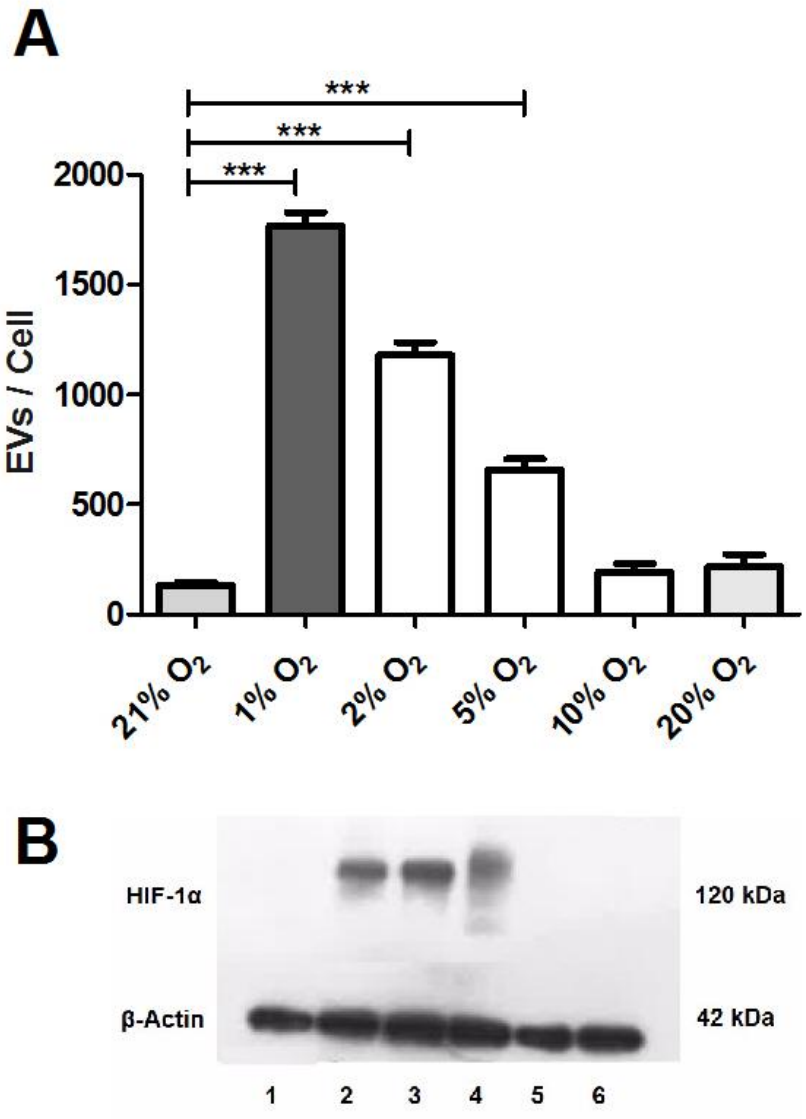

647

Figure 2. The effect of hypoxia on EV size distribution. Assessed in 50 nm bin sizes, results represent [n = 5]. Each sample was analysed in quintuplicate and the mean was used in further analysis. Data are expressed as mean ± SEM. *** reflects p< 0.001.

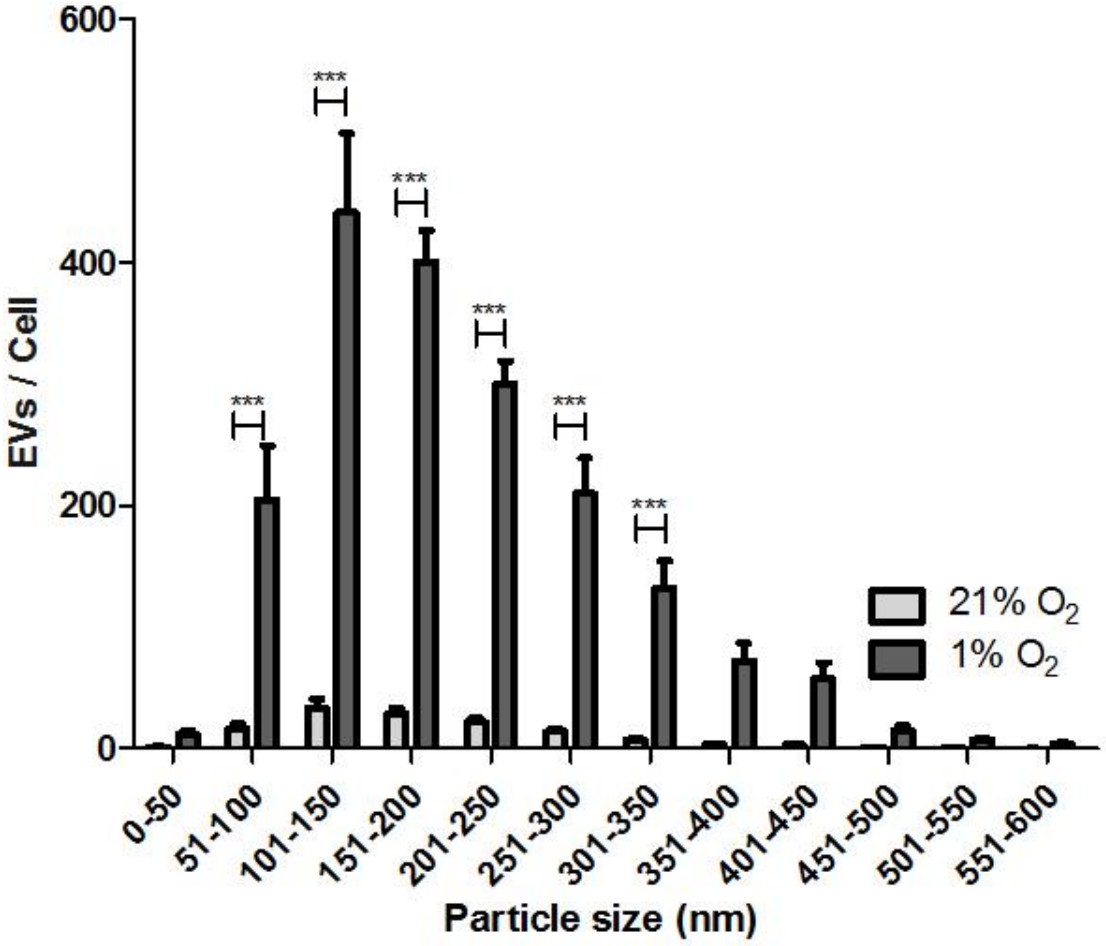

Figure 3. The effect of the hypoxia mimetic agent desferrioxamine on EV production. (A) EVs produced per cell. (B) Western blot confirming successful stabilisation of HIF-1α in normoxia. Lane 1: 1% O_2. Lane 2: 1% O_2 + DFO. Lane 3: 21% O_2. Lane 4: 21% O_2 + DFO. Results represent [N=5]. Each sample was analysed in quintuplicate and the mean was used in further analysis. Data are expressed as mean ± SEM. *** and * reflect p< 0.001.

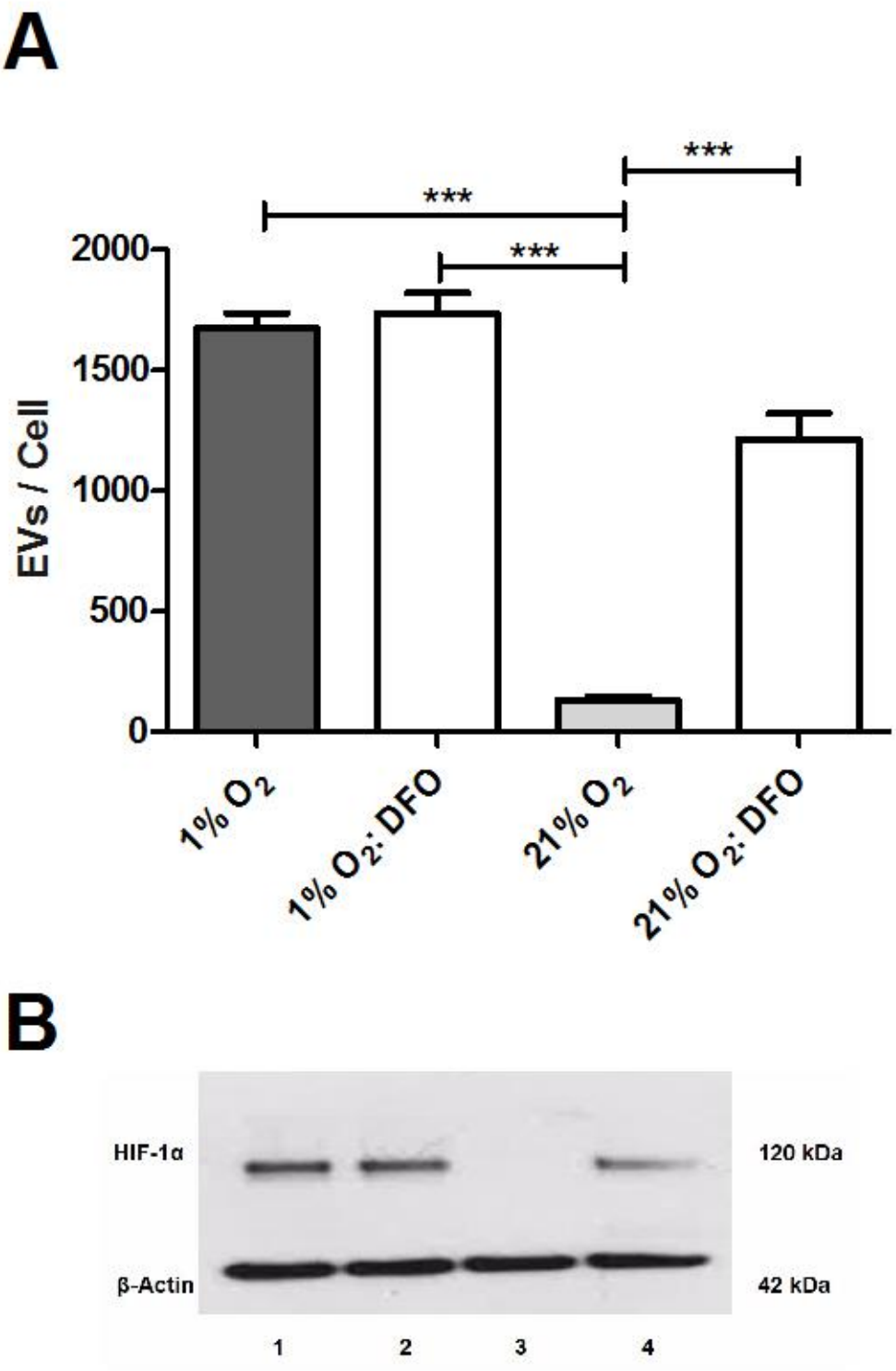

Figure 4. The effect of silencing HIF-1α and HIF-2α on EV production. (A) HIF-1α siRNA; EVs produced per cell. (B) HIF-2α siRNA; EVs produced per cell. (C) Western blot confirming successful silencing of HIF-1α. Lane 1: 21% O_2. Lane 2: 1% O_2. Lane 3: 1% O_2, HIF-1α siRNA. Lane 4: 1% O_2, control siRNA. (D) Western blot confirming successful silencing of HIF-2α. Lane 1: 21% O_2. Lane 2: 1% O_2. Lane 3: 1% O_2, HIF-2α siRNA. Lane 4: 1% O_2, control siRNA. Results represent [n = 5]. Each sample was analysed in quintuplicate and the mean was used in further analysis. Data are expressed as mean ± SEM. *** reflects $p < 0.001$.

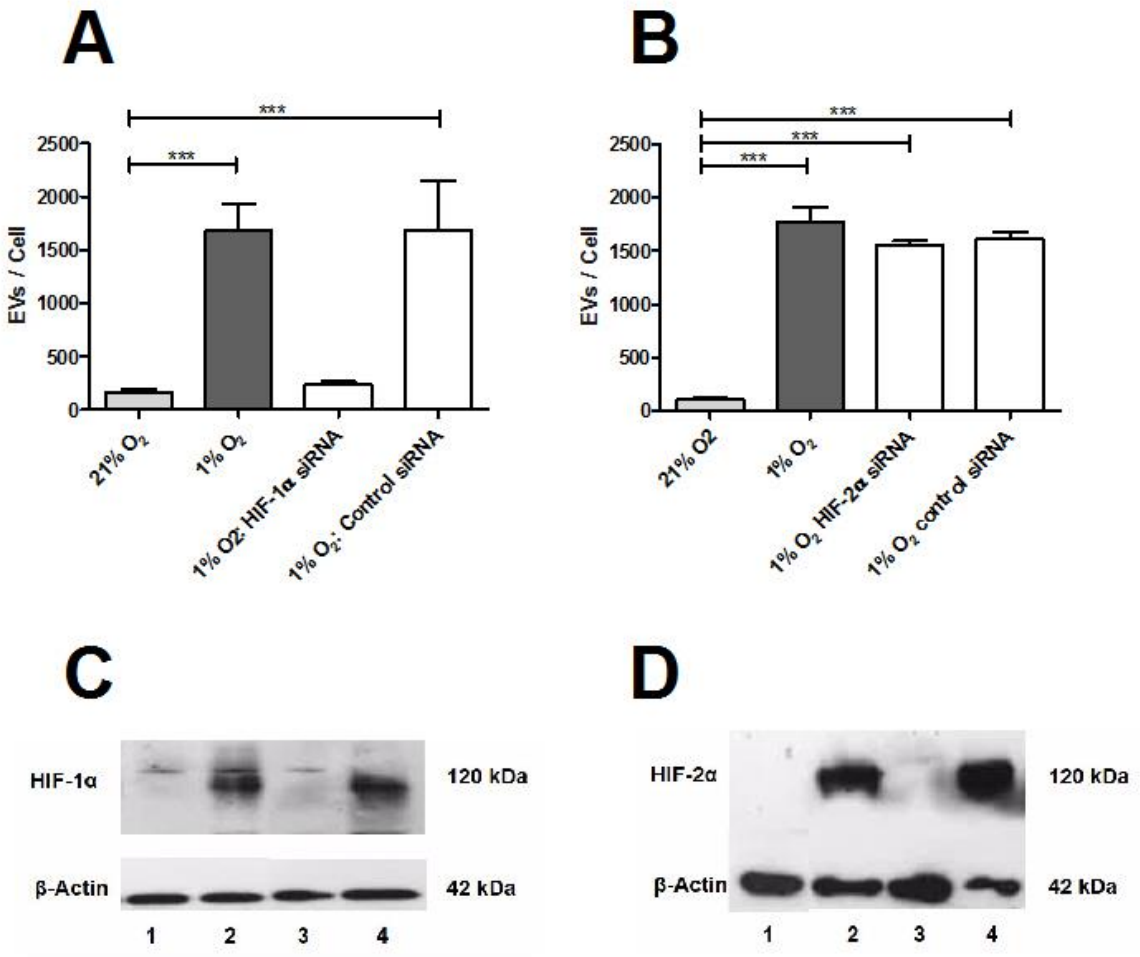

Figure 5. The effect of sodium nitrite on EV production. (A) EVs produced per cell following exposure to various conditions. (B) Western blotting showing the expression of HIF-1α under various conditions. Lane 1: 21% O_2. Lane 2: 21% O_2, $NaNO_2$. Lane 3: 1% O_2. Lane 4: 1% O_2, $NaNO_2$. Lane 5: 1% O_2, $NaNO_2$ and allopurinol. Results represent [n = 5]. Each sample was analysed in quintuplicate and the mean was used in further analysis. Data are expressed as mean ± SEM. **, *** reflects p< 0.01, and p< 0.001 respectively.

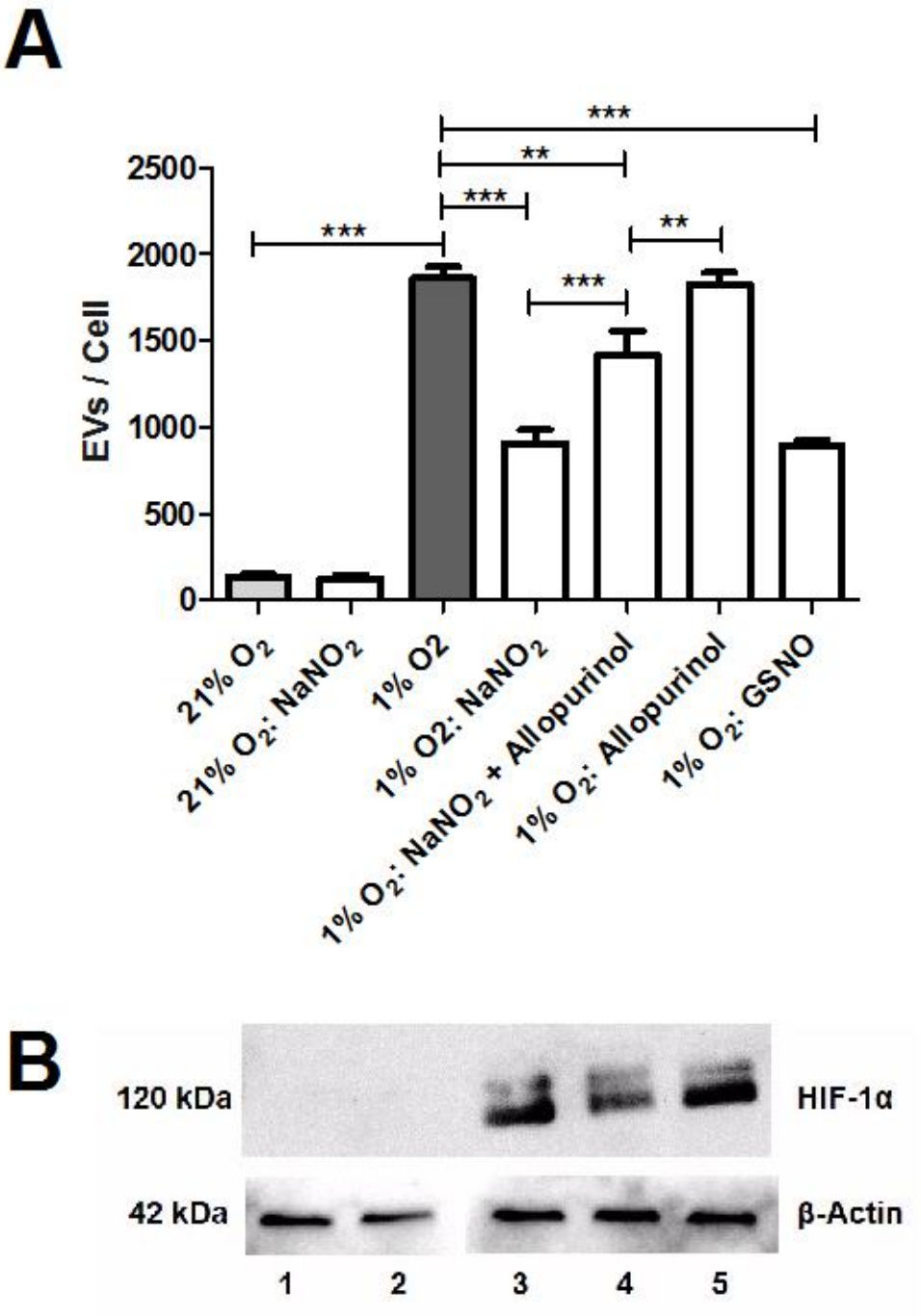

Figure 6. The effect of hypoxia and sodium nitrite on EV production in HUVECs. (A) EVs produced by HUVECs following exposure to hypoxia and/or $NaNO_2$. (B) Western blotting showing the expression of HIF-1α following exposure to hypoxia and/or $NaNO_2$. Lane 1: 1% O_2. Lane 2: 1% O_2 + $NaNO_2$. Lane 3: 21% O_2. Lane 4: 21% O_2 + $NaNO_2$. Results represent [n=5]. Each sample was analysed in quintuplicate and the mean was used in further analysis. Data are expressed as mean ± SEM. *** reflects $p< 0.001$.